

Blueprint for efficient nuclear spin characterization in color center

Majid Zahedian,¹ Vadim Vorobyov,^{1,*} and Jörg Wrachtrup^{1,2}

¹3rd physical institute University of Stuttgart, Germany

²Max Planck Institute for solid state physics, Stuttgart, Germany

(Dated: October 31, 2023)

Nuclear spins in solids is one of the most promising platforms for realisation of a scalable quantum hardware. They could be efficiently addressed at single site level by nearby single colour centers via the spin resonance. However, characterising each nuclear spin is quite cumbersome as the characterisation protocol may differ depending on the strength of the hyperfine coupling. The most adopted protocol is modified electron spin Hahn-echos such as CPMG and XY8 pulse sequences. In some cases, e.g. for spin 1/2, strongly coupled spins, and bispecies bath, this protocol contains severe problems in applying for the nuclear spin bath characterisation. Here, we present a more straight forward method to obtain hyperfine interaction among nuclear spins and the electron spin. This method can be used for a variety of platform including emerging S=1/2 group IV defects in diamond (e.g. SiV, GeV, SnV, PbV) or Silicon vacancy in Silicon Carbide. We summarize theoretical framework and adopt it from ESR for the use in colour centers with various spins, and numerically consider case of nuclear spin cluster, as compare performance of various protocols on this example via the Fisher information matrix.

I. INTRODUCTION AND BACKGROUND

Optically active defects in solids, color centers, has been applied for realising different quantum applications [1], such as a quantum network [2], quantum sensing [3], and quantum registers [4].

Each center contains an electron spin that can be controlled directly with microwaves, initialised and read out via optical excitation. The key element for most applications is that they could be coupled through the hyperfine coupling to the bath of numerous nuclear spins presenting a long living quantum memories and could present an optically accessible nuclear spin qubit register. To design the efficient quantum control for the memories, a precise knowledge of the full hamiltonian of the register needs to be known and characterised before. However, characterising the nuclear spin hyperfine coupling could be a challenging and a lengthy procedure [? ?]. Traditionally, nuclear spin characterisation is done with Optically Detected Magnetic Resonance (ODMR) [? ? ?], however the spectroscopic resolution is limited to the $1/T_2^*$ of the electron spin. Hahn Echo type sequences have been used to refocus the electron spin and enhance the coherence time of the electron spin [5] thus improving the resolution to $1/T_2$. This method could be applied for the defects with a specific nuclear spins configuration (which?). In particular, the certain relation to the magnetic field and the coupling of the nuclear spins should be kept, (weakly coupled nuclear spins), as well as the spin number of the electron spin is affecting the observed behaviour. Depending on the applied protocol for the nuclear spins characterisation, the number of accessible nuclear spin can increase. Electron Spin Echo Envelop Modulation (ESEEM) types of sequences allow

us to access the highest number of nuclear spins since the spectroscopy resolution is limited to the longitudinal relaxation time (T_1) of the system (see fig. 1) [? ?]. In particular we consider following common examples of nuclear spin registers ubiquitous in the applications. First, NV-like case with S=1, and weakly coupled nuclear spins, at high magnetic field such that $\gamma_n B \gg A_{zx}$. This case is very well studied in the works of [? ? ? ? ?]. The ability to see narrow peaks with analytically predictable position and contrast allows one to solve the inverse problem of characterising the coupling of the nuclear spins to the electron spins. The second case (see in Fig. 1b) refers to a similar case but with a strongly coupled nuclear spin, which hinders the observation of a weakly coupled nuclear spins. This case in particular is relevant for the case, where additional to the weakly coupled register a strongly coupled nuclear spin is used for e.g. repetitive enhancement of the readout, via using the strongly coupled ancilla resolved in electron spin resonance spectra. The third case (Fig. 1c) is relevant for the S=1/2 case, where due to the lack of the offset in the average evolution of the nuclear spin, its dynamics weakly depends on the A_{zz} and only in the second order on the A_{zx} [?]. This leads to a poor distinguishing ability of multiple nuclear spins and as a result lack of individual addressability of nuclear spins. Finally, in the case of other materials host platforms, a bispecies nuclear spin bath could be observed, where the resonance peaks referring to different Larmour frequencies of different species additionally complicate the reconstruction of the hamiltonian, and for unambiguous reconstruction of the interactions, additional measurements e.g. at different B field would be needed. In this work we argue that a correlation type sequence, based on 5p esem, could serve as a general framework as it promises great reconstruction potential for all above-mentioned cases.

* v.vorobyov@pi3.uni-stuttgart.de



FIG. 1. Comparing DD and ESEEM as two nuclear spin characterisation method in different systems. a. An electron spin one system: in DD signal, each nuclear spin has a distinct resonance time up to first order of A_{zz} ; the accuracy of the obtained hyperfine interaction is limited to T_2 of the electron spin. In the Fourier transform of the ESEEM signal, the two resonance frequency of each spin is present; the accuracy of the obtained hyperfine interaction is limited to T_1 of the electron spin. b. An electron spin one system with two strongly coupled nuclear spins and many weakly coupled spins. No resonance time is detectable since the required condition for DD ($\omega_L \gg A_{zz}, A_{zx}$) does not hold. However, resonant frequencies is still obtainable in the ESEEM signal. c. An electron spin one half system: nuclear spins have more or less the same resonance time as it depends on the second order of hyperfine coupling. However, resonant frequency of each spins is distinguishable in the ESEEM signal. d. A system containing two different nuclear spin species: two nuclear spin bath can interfere in the DD signal, which makes the signal analysis more challenging. However, the species can be inferred from ESEEM signal since species have different Larmour frequencies.

II. RESULTS

We consider a central spin system of *non-interacting* nuclear spins $I = 1/2$ coupled to the central electron spin S . The central electron spin is manipulated resonantly with the microwave pulses, which transfer the population between the two sublevels, denoted as $m_s = s_0$ and $m_s = s_1$. These two spin sublevels are separated, due to the Zeeman effect and/or zero field splitting, and form an two-level subsystem with energy splitting of ω_a . The Hamiltonian of the system in the secular approximation

and in the rotating frame of the applied microwave ω_{mw} can be written as:

$$H = \Delta S_z + \sum_k (\omega_L^{(k)} + A_{zz}^{(k)} S_z) I_z^{(k)} + A_{zx}^{(k)} S_z I_x^{(k)} \quad (1)$$

Where $\Delta = \omega_a - \omega_{mw}$ is the detuning, $\omega_L^{(k)} = \gamma_n^{(k)} B$ is nuclear Rabi frequency with $\gamma_n^{(k)}$ nuclear spin gyromagnetic ratio and B external magnetic field, A_{zz}, A_{zx} parallel and perpendicular secular component of hyperfine tensor. The Hamiltonian is diagonal in the electron spin subspace, thus the hamiltonian for the nuclear

spins could be rewritten in electron spin subdomains s_i ($i = 0, 1$). The nuclear spin hamiltonian could be solved for eigenenergies, which determine the precession frequencies of $\omega_i = \sqrt{(\omega_L + s_i A_{zz})^2 + (s_i A_{zx})^2}$, $i = 0, 1$ along the eigenvector axes $\vec{n}_i = (\frac{s_i A_{zx}}{\omega_i}, 0, \frac{\omega_L + s_i A_{zz}}{\omega_i})$. It is assumed that the pulse duration t_p are short enough ($\omega_L t_p \ll 1$) that the nuclear spin dynamics during this time is negligible. For completeness we start our analysis with the simplest characterization sequence, which is the electron spin Ramsey sequence (free induction decay of electron) (see Appendix for derivation). The Ramsey signal can be obtained as follows:

$$\langle \sigma_z \rangle_{Ram} = \cos(\Delta\tau) \prod_{k=1}^n \left[\cos\left(\frac{\omega_0\tau}{2}\right) \cos\left(\frac{\omega_1\tau}{2}\right) + (\vec{n}_0 \cdot \vec{n}_1) \sin\left(\frac{\omega_0\tau}{2}\right) \sin\left(\frac{\omega_1\tau}{2}\right) \right]^{(k)} e^{-\left(\frac{\tau}{T_2^*}\right)^m} \quad (2)$$

We do not take any relaxation process into account and the gray exponential decay is put by hand to remember the relaxation time scale. Ramsey signal decay with electron spin T_2^* , so it can be used to observe the core of the defect. Ramsey sequence is sensitive to detuning since the electron spin is not refocused, however it is possible to sense nuclear spins with vanishing perpendicular hyperfine coupling.

To enhance the relaxation time and have access to more nuclei, one can add a π pulse in between the Ramsey sequence and create Hahn-echo sequence and obtain the following signal:

$$\langle \sigma_z \rangle_{HE} = \prod_{j=1}^n \left[1 - 2k^2 \sin^2\left(\frac{\omega_0\tau}{2}\right) \sin^2\left(\frac{\omega_1\tau}{2}\right) \right]^{(j)} e^{-\frac{2\tau}{T_2}} \quad (3)$$

Where $k = \frac{(s_1 - s_0)\omega_L A_{zx}}{\omega_0\omega_1}$ is the modulation amplitude of each nuclear spin. Without any nuclear spin, Hahn Echo sequence creates the electron spin echo signal with the envelope of stretched exponential decay with T_2^{HE} . However in the presence of nuclear spins, the electron spin echo envelope will be modulated due to interaction with nuclei. Hence, this sequence also called Electron Spin Echo Envelope Modulation or shortly ESEEM. Even though the coherence time is increased, distinguishing the effect of different nuclear spins in the total signal is very complicated. Hahn Echo sequence can be used for defects that contain a few strongly coupled nuclei. In order to differentiate the resonance frequency of each nuclear spin or make the oscillation sharper, one can to add more π pulses and for the so-called Dynamical Decoupling sequence to sharpen the resonance conditions (neglecting decoherence terms):

$$\langle \sigma_z \rangle_{DD} = \prod_{j=1}^n \left[1 - 2k^2 \sin^2\left(\frac{\omega_0\tau}{2}\right) \sin^2\left(\frac{\omega_1\tau}{2}\right) \frac{\sin^2\left(\frac{N\theta}{2}\right)}{\cos^2\left(\frac{1}{2}\theta\right)} \right]^{(j)} e^{-\frac{2N\tau}{T_2(N)}} \quad (4)$$

Where

$$\theta = \arccos \left[\cos(\omega_0\tau) \cos(\omega_1\tau) - \vec{n}_0 \cdot \vec{n}_1 \sin(\omega_0\tau) \sin(\omega_1\tau) \right] \quad (5)$$

$\vec{n}_0 \cdot \vec{n}_1 = \frac{\omega_L^2 + (s_0 + s_1)A_{zz} + s_0 s_1 (A_{zz}^2 + A_{zx}^2)}{\omega_0\omega_1}$ and N is the number of π pulses that must be an even. Each nuclear If the magnetic field is high or all nuclear spins are weakly coupled such that $\omega_L \gg A_{zz}, A_{zx}$, the multiplication rule can be approximated by a summation rule, which makes the higher order resonance disappear:

$$\langle \sigma_z \rangle_{DD} \approx 1 - 2 \sum_{j=1}^n \left[k^2 \sin^2\left(\frac{\omega_0\tau}{2}\right) \sin^2\left(\frac{\omega_1\tau}{2}\right) \frac{\sin^2\left(\frac{N\theta}{2}\right)}{\cos^2\left(\frac{1}{2}\theta\right)} \right]^{(j)} e^{-\frac{2N\tau}{T_2(N)}} \quad (6)$$

The parallel component of the hyperfine interaction can be obtained from the resonance time of each nuclear spin:

$$\tau_p \approx \frac{(2p+1)\pi}{\omega_0 + \omega_1} \approx \frac{(2p+1)\pi}{2\omega_L \left(1 + \frac{s_0 + s_1}{2} \frac{A_{zz}}{\omega_L} + \frac{s_0^2 + s_1^2}{4} \frac{A_{zx}^2}{\omega_L^2}\right)} \quad (7)$$

The perpendicular part of hyperfine interaction can be obtained from a fit to the Lorentzian dip with the width of $\frac{(s_1 - s_0)\omega_L A_{zx}}{(2p+1)\pi\omega_0\omega_1}$ or varying the number of pulses and fitting the minima position to the formula $\langle \sigma_z \rangle_{DD} \approx 1 - 2 \sin^2\left(\frac{N}{2} \frac{(s_1 - s_0)\omega_L A_{zx}}{\omega_0\omega_1}\right)$. Although Dynamical Decoupling (DD) sequence is well understood and used to characterize nuclear spins, it is not applicable for any system. First, DD only works for defects with high magnetic field and low hyperfine coupling ($\omega_L \gg A_{zz}, A_{zx}$). Second, the signal is limited to electron spin T_2 , which is difficult to make it equal to T_1 . Third, the signal analysis is rather complicated and time-consuming. (Maybe AI solves this problem in the future?) one has to collect enough data to make sure no two nuclear spin overlap in the signal. Forth, this sequence does not work for spin one half system, e.g., group IV defect in diamond, since parallel component of hyperfine coupling cancels their effect in the resonance time up to the first and second order. Hence, the resonance time depends on the second order of perpendicular component. In this work, we take 23 nuclear spin characterized in paper [6] as a realistic case. In this work, we take the 23 nuclear spins cluster characterized in paper [6] as a realistic case. First, we apply this to the dynamical decoupling sequence, and visualise the obtained results. Fig 2 compares DD signal for the same nuclear spin register but different defects in diamond. An intuitive description for the sensitivity of a sequence to the variation of hyperfine coupling could be estimated knowing the width and sensitivity of the position of the resonances. First, we consider the case of NV center in diamond. The width of a dip $\delta\tau = \frac{1}{\omega_L}$ and taking the derivative of the resonance time, we define the sensitivity of longitudinal hyperfine coupling as follows:

$$\delta A_{zz} = \frac{\delta\tau}{\left| \frac{\partial \tau_k}{\partial A_{zz}} \right|} = \frac{2}{\tau_k} \frac{A_{zx}}{\omega_L} \geq \frac{4}{T_2^{HE}} \frac{A_{zx}}{\omega_L} \quad (8)$$

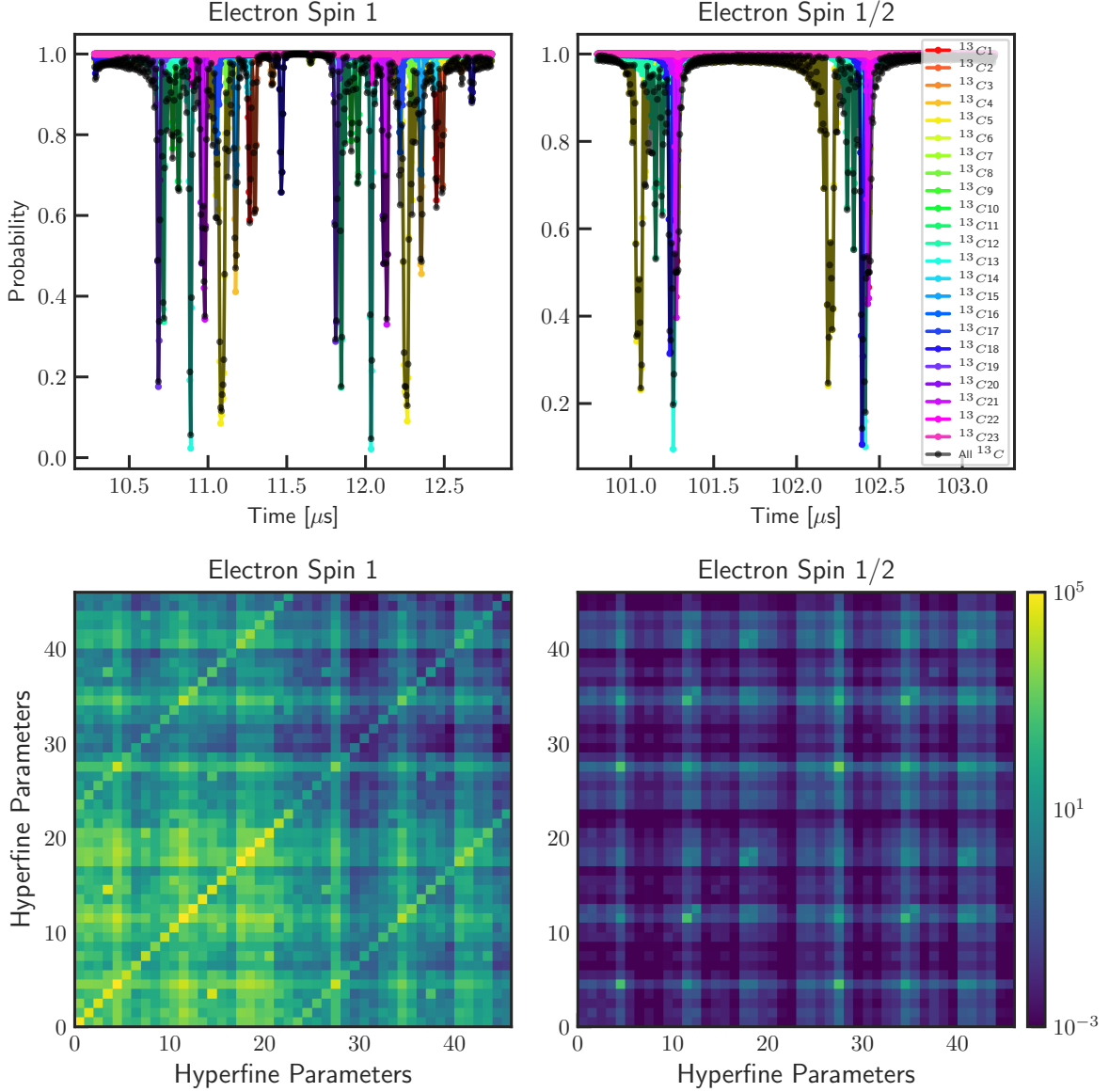


FIG. 2. Simulated DD signal with 64 π -pulses for the register reported [6] assuming the electron spin is a. spin one b. spin one-half system. Simulated Fisher information matrix for the case of the electron spin c. one d. one-half system.

If we assume the typical values of $T_2^{HE} = 100 \mu\text{s}$ and $\omega_L = 500 \text{ kHz}$, a weakly coupled nuclear spin $A_{zx} = 5 \text{ kHz}$ can be distinguished from another weakly coupled nuclear spin with $\delta A_{zz} = 400 \text{ Hz}$. For $S = 1/2$, e.g. for group IV defects in diamond, the resonance times is sensitive to the second order of A_{zx} and no sensitivity to A_{zz} . Hence, even at large τ the resonances related to nuclear spins will not be separated well. We define the sensitivity for the spin one half system as follows:

$$\delta A_{zx} = \frac{\delta\tau}{\left| \frac{\partial\tau_k}{\partial A_{zx}} \right|} = \frac{4}{\tau_k} \geq \frac{8}{T_2^{HE}} \quad (9)$$

Assuming the typical values of $T_2^{HE} = 100 \mu\text{s}$, a nuclear spin can be distinguished from another one if their transverse hyperfine coupling is separated by $\delta A_{zx} = 80 \text{ kHz}$, which is quite inaccurate and ≈ 160 times worse than for $S = 1$. To quantify the difference in sensitivity to estimating the hyperfine parameters, we perform calculation of the Fisher information matrix (FIM) for the 23 nuclear spin cluster, with 23 A_{zz} and 23 A_{zx} parameters (see Fig. 2c,d). The fisher information matrix is estimated for the probability to measure state $|0\rangle$ and reads as:

$$F_{ij}(\mathbf{A}) = \sum_{\tau} \frac{\partial p(0, \tau, \mathbf{A})}{\partial A_i} \frac{\partial p(0, \tau, \mathbf{A})}{\partial A_j} \frac{1}{p(1-p)}. \quad (10)$$

For the typical case of NV center, with $S = 1$, since all the nuclear spin resonances are clearly resolved, the Fisher information matrix takes a diagonal shape, revealing a low covariance between the various nuclear spin resonances. The crosstalk is existing between A_{zz} and A_{zx} of same nuclear spin, which is because the position of the peaks depends on both values. The fisher information gives a bound for the precision of parameter estimation, known as Cramér–Rao bound:

$$\delta A^2 \geq \frac{1}{F(A)N} \quad (11)$$

For the presented protocol, the precision for various spins is limited by 0.09 Hz ~~Hz squared?~~ for the $S=1$, for the $N = 4000$, while for the $S=1/2$ the value of the Cramer-Rao bound reads as ~~XXX~~ which is ~~YYYY~~ time smaller.

The striking difference to the $S = 1$ fisher information matrix, is the behaviour of the defect with $S = 1/2$. First of all, for both spin $S=1/2$ and $S=1$, the sequence spectral resolution is limited with T_1 relaxation time of the electron spin. On the other hand, a sequence sensitivity is limited by T_2 . The main principle of 5-pulse ESEEM [7] is to create an entanglement (via e.g. Hahn-echo or CPMG block) before the free evolution of the nuclear spins and after make a second correlating sequence. In other words, change the initial density matrix for the Ramsey sequence from such that entanglement already exist in the electron polarization terms of the density matrix, thus limited by T_1 time. Fig 5 shows the sequence, which can be interpreted as two Hahn Echos that are separated by a long free evolution $T \gg T_2^*$ such that the coherence of the electron spin vanishes. The analytical formula to this sequence is provided in the appendix B. During the free evolution time, each nuclear spins oscillates with either of two resonance frequencies obtained from eq. 1.

Fig 3 shows the Fourier transform of the signal. Zooming into area close to the Larmor frequency reveals the weakly coupled nuclei. Each nuclear spins have two peaks in the spectrum referring to the ω_a and ω_b . Expanding the resonance frequencies up to first order with respect to hyperfine coupling ~~results that the weakly coupled nuclei keep their order as they go further away from the nuclei.~~ This fact makes their characterisation rather straight forward. To observe the weakly coupled nuclei more pronouncedly, one can use ~~DD~~-ESEEM sequence by adding more π pulses in the entangling periods. To distinguish other nuclei, extra measurements ~~is~~ required. One method is to use two dimensional hyperfine correlation spectroscopy (2D Hyscore) [8]. However, this method is rather time-consuming as two time variables has to be swept. The optimum time sampling techniques might be used to optimise the time of 2D sampling. Here we suggest an alternative way, which in conventional ESR is used, i.e. sweeping τ parameter and keep the track of frequency amplitude as a function of τ . Two frequencies that belong to the same nuclear are correlated because the modulation depth oscillates with blind spot terms

of both frequencies $\sin^2(\frac{\omega_0\tau}{2})\sin^2(\frac{\omega_1\tau}{2})$. Fig. 4 shows two frequencies goes to bright and blind spots simultaneously. Hence, taking two dimensional correlation of the spectrum, one can deduce which two frequencies are correlated and belong to the same nuclear.

To simulate the realistic experimental situation we model the electron spin state is projected to 0 and 1 with a binomial distribution where the probability determined by the analytical expressions. Then, we assume the bright (dark) state emits 3 (0.1) photons on average with a Poissonian distribution. We repeat the measurement at each point for 10000 times to reduce the classical photon shot noise.

Next we approach estimation of number of nuclear spins, which could be identified. It depends on the duration of free evolution time and the choice of inter-pulse timing τ .



III. DISCUSSION

Here is the concise conclusion @Vadim



ACKNOWLEDGMENTS

We acknowledge financial support by European Union's Horizon 2020 research and innovation program ASTERIS under grant No. 820394, European Research Council advanced grant No. 742610, SMel, Federal Ministry of Education and Research (BMBF) project MiLi-Quant and Quamapolis, the DFG (FOR 2724), the Max Planck Society, and the Volkswagenstiftung. M.Z. thanks Max Planck School of Photonics for financial support.

Appendix A: Sequences

The details of mentioned sequences in the main text can be found in fig 5:

Appendix B: 5pESEEM formula

Here we need to define a few unitary operators/ The evolution in the first Hahn-echo is given by V operators, the middle free evolution is given by F operators, and the second Hahn-echo is given by W operators:

$$V_0 = U_0(\tau_1)U_1(\tau_1), \quad V_1 = U_1(\tau_1)U_0(\tau_1) \quad (B1)$$

$$F_0 = U_0(T), \quad F_1 = U_1(T)U_0 \quad (B2)$$

$$W_0 = U_0(\tau_2)U_1(\tau_2), \quad W_1 = U_1(\tau_2)U_0(\tau_2) \quad (B3)$$

The signal can be obtained from four different types of trajectories that the electron spin can take. We use the fact that multiplication of unitary operators is also a unitary operator and every unitary in spin one half space can be written in terms of a rotation angle, axis,

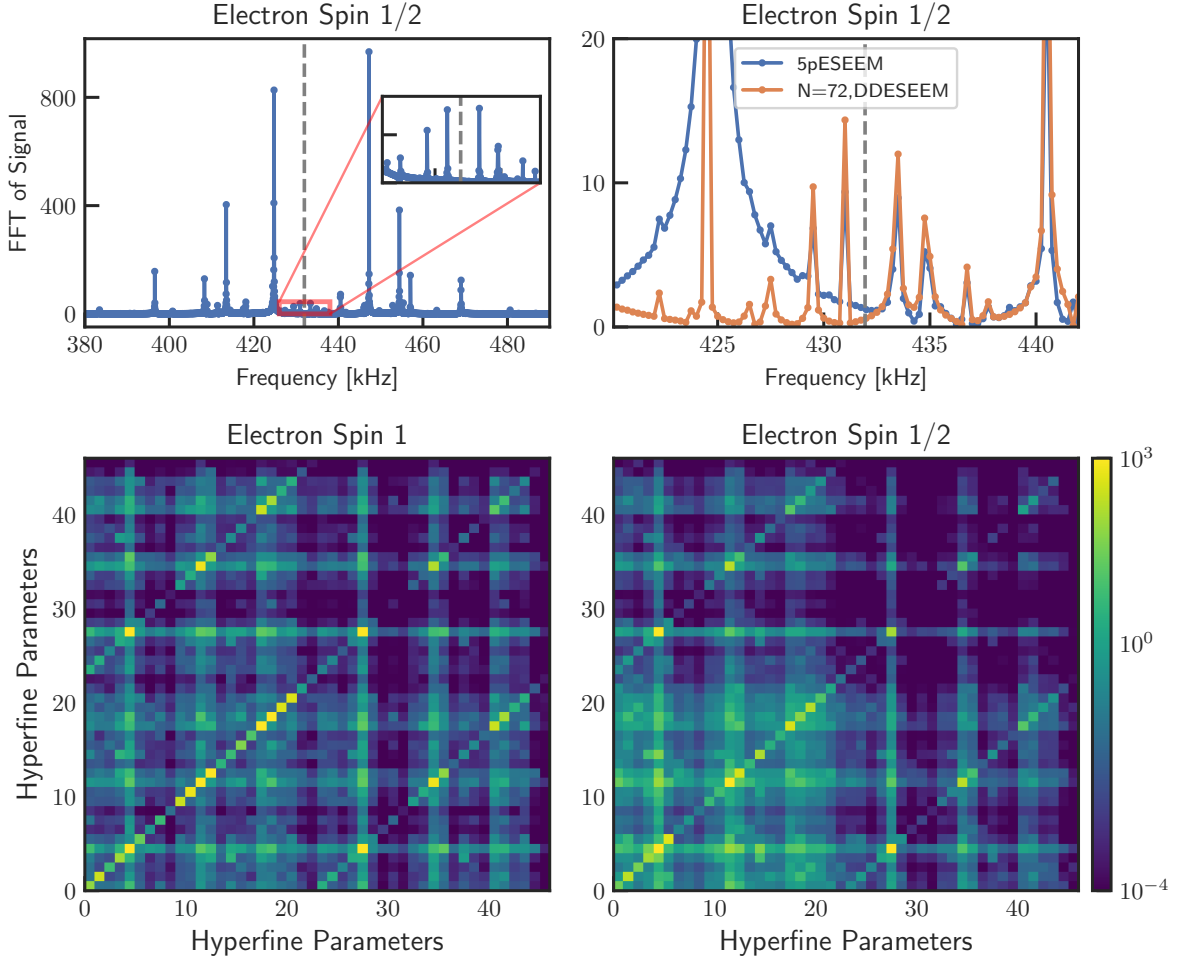


FIG. 3. Simulated FFT of ESEEM signal with a zoom into weakly coupled nuclear spins for the register reported [6] assuming the electron spin is one-half. b. Enhancing the sensitivity to weakly coupled spins by increasing number of π -pulses to $N = 72$ pulses in each entangling period. τ is set to the Larmor bright spot. Simulated Fisher information for the case of the electron spin c. one d. one-half system.

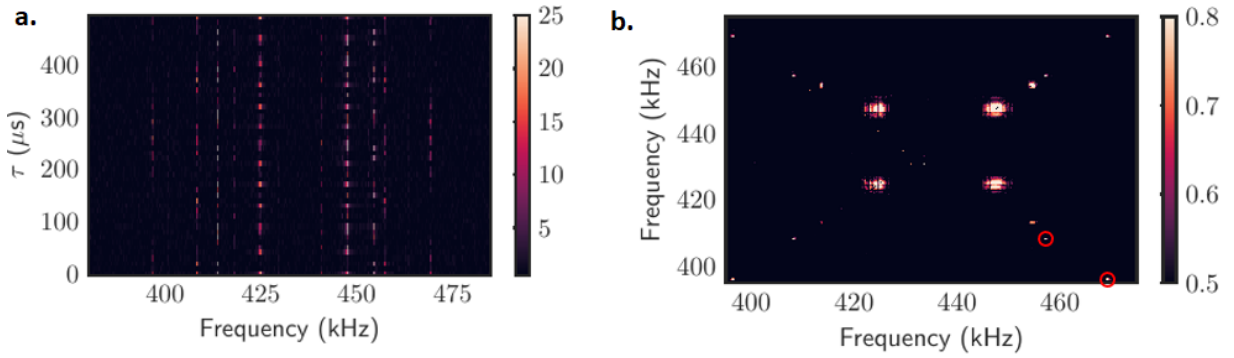


FIG. 4. a. FFT of ESEEM signal for τ from 10 μ s to 500 μ s with the step of 10 μ s b. 2D correlation of each frequency for different τ .

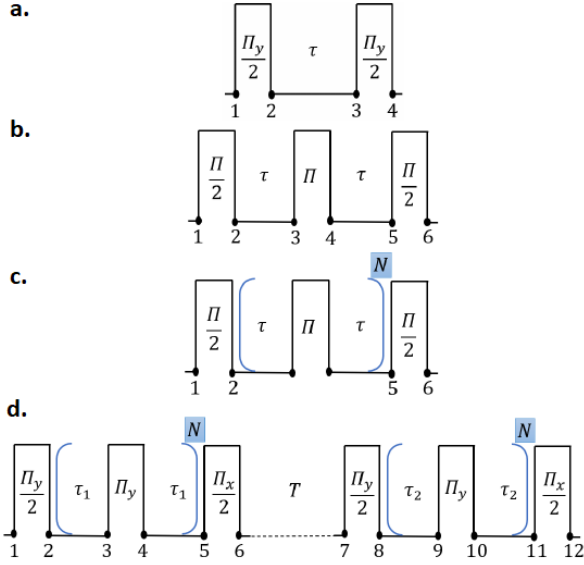


FIG. 5. Pulse sequences a. Ramsey b. Hahn Echo c. Dynamical Decoupling d. DDESEEM

and Pauli Matrices $\vec{\sigma}$. We denote the unitary operator $U = \exp(-i\theta_U \hat{n}_U \cdot \vec{\sigma}) = M \cos(\theta_U) \mathbf{I} - i \sin(\theta_U) \hat{n}_U \cdot \vec{\sigma}$. The signal for 5-pulse ESEEM can be obtained as follows:

$$\begin{aligned} \langle \sigma_z \rangle_{5p} = & \frac{1}{4} \left(\prod_{j=1}^n [\cos(\theta_{W_1 F_1 V_0 V_1^\dagger F_1^\dagger W_0^\dagger})]^{(j)} \right. \\ & - \prod_{j=1}^n [\cos(\theta_{W_1 F_1 V_1 V_0^\dagger F_1^\dagger W_0^\dagger})]^{(j)} \\ & + \prod_{j=1}^n [\cos(\theta_{W_1 F_0 V_0 V_1^\dagger F_0^\dagger W_0^\dagger})]^{(j)} \\ & \left. - \prod_{j=1}^n [\cos(\theta_{W_1 F_0 V_1 V_0^\dagger F_0^\dagger W_0^\dagger})]^{(j)} \right) e^{-\frac{2\tau_1 + 2\tau_2}{T_2} - \frac{T}{T_1}} \quad (B4) \end{aligned}$$

Multiplying the matrices and finding the rotation angles gives the expectation value of σ_z for 5pESEEM sequence as it can be found in this article [7]:

$$\langle \sigma_z \rangle_{5p} = \frac{1}{4} \left(\prod_{j=1}^n E_{\alpha_+}^{(j)} - \prod_{j=1}^n E_{\alpha_-}^{(j)} + \prod_{j=1}^n E_{\beta_+}^{(j)} - \prod_{j=1}^n E_{\beta_-}^{(j)} \right) \quad (B5)$$

Where each term can be calculated as follows:

$$\begin{aligned} E_{\alpha_\pm}^{(k)} = & E_{2p}(\tau_1) E_{2p}(\tau_2) \mp B \left(-4k^2 C_\alpha \right. \\ & + 4k \cos^4(\eta) \cos(\omega_\alpha T + \phi_{\alpha_+} + \phi_{\beta_+}) + 2k^2 \cos(\phi_{\beta_-}) \cos(\omega_\alpha T + \phi_{\alpha_+}) \\ & \left. + 4k \sin^4(\eta) \cos(\omega_\alpha T + \phi_{\alpha_+} - \phi_{\beta_+}) \right) \quad (B6) \end{aligned}$$

E_{2p} is 2-pulse ESEEM sequence signal:

$$\begin{aligned} E_{2p}(t) = & \left(1 - \frac{k}{2} \right) + \frac{k}{2} \left(\cos(\omega_\alpha t) + \cos(\omega_\beta t) \right. \\ & \left. - \frac{1}{2} \cos(\omega_- t) - \frac{1}{2} \cos(\omega_+ t) \right) \quad (B7) \end{aligned}$$

With $\omega_\pm = \omega_\alpha \pm \omega_\beta$, B is the blind spot term and C_α is a constant term:

$$\begin{aligned} B = & \sin\left(\frac{\omega_\alpha \tau_1}{2}\right) \sin\left(\frac{\omega_\alpha \tau_2}{2}\right) \sin\left(\frac{\omega_\beta \tau_1}{2}\right) \sin\left(\frac{\omega_\beta \tau_2}{2}\right) \quad (B8) \\ C_\alpha = & \cos\left(\frac{\omega_\alpha \tau_1}{2}\right) \cos\left(\frac{\omega_\alpha \tau_2}{2}\right) \sin\left(\frac{\omega_\beta \tau_1}{2}\right) \sin\left(\frac{\omega_\beta \tau_2}{2}\right) \quad (B9) \end{aligned}$$

The resonance frequencies are $\omega_{\alpha(\beta)} = \sqrt{(\omega_L + s_{0(1)} A_{zz})^2 + (s_{0(1)} A_{zx})^2}$. The quantization axis of nuclear spins is tilted by $\eta_{\alpha(\beta)} = \arctan\left(\frac{s_{0(1)} A_{zx}}{\omega_L + s_{0(1)} A_{zz}}\right)$, which gives the parameter $\eta = \frac{\eta_\alpha - \eta_\beta}{2}$. The modulation depth of each nuclear spin is $k = \sin^2(2\eta) = \left(\frac{(s_1 - s_0) \omega_L A_{zx}}{\omega_\alpha \omega_\beta}\right)^2$, the phase shifts are $\phi_{\alpha\pm} = \frac{\omega_\alpha(\tau_1 \pm \tau_2)}{2}$ and $\phi_{\beta\pm} = \frac{\omega_\beta(\tau_1 \pm \tau_2)}{2}$. The two expression for the β pathways can be obtained by exchanging α and β in equation B6, B8, and B9.

As we have shown, the signal from the register comes from the multiplication of signals from individual nuclear spins. Hence, if the modulation depth is not low (low magnetic field condition), the second or higher order frequencies will appear in the spectrum. So, the product rule lead to the creation of inter-nuclear peaks at multi-quantum frequencies that can be sums or subtraction of single quantum frequencies of various nuclei. Nevertheless, the multiple quantum resonance peaks are informative for the electron spin one half system because one can deduce that two peaks that are added or subtracted belong to the same electron spin manifold; Hence it is possible to get the relative phase of nuclei. Another consequence of the product rule is the cross-suppression effect, which means the presence of strongly coupled nuclei suppress the amplitude of weakly coupled nuclei while weakly coupled ones do not suppress the amplitude of strongly coupled nuclei [9]. However, if we assume the Larmor frequency is relatively high or the modulation depth is low, both of these effect will vanish as the product rule can be approximated by a summation rule:

$$\begin{aligned} E_\alpha = & \prod_{j=1}^n E_{\alpha_+}^{(j)} - \prod_{j=1}^n E_{\alpha_-}^{(j)} \\ \approx & \sum_{j=1}^n \left[-8Bk \cos^4(\eta) \cos(\omega_\alpha T + \phi_{\alpha_+} + \phi_{\beta_+}) \right]^{(j)} \quad (B10) \end{aligned}$$

The blind spot term shows that how this sequence can be engineered to increase or reduce the signal amplitude

of one nuclear spin from the spectrum. The bright and blind spots of a frequency in the spectrum are as follows:

$$\text{Blind Spots: } \tau = \text{even} \frac{\pi}{\omega} \quad (\text{B11})$$

$$\text{Bright Spots: } \tau = \text{odd} \frac{\pi}{\omega} \quad (\text{B12})$$

The blind spots does not depend only on one frequency but on the nuclear spin. It means if one resonant frequency is blinded, the other resonant frequency and all the multiple quantum resonances also vanishes. This can be used as a manifestation that which two peaks are from one nuclei. Also, This is very helpful especially in the presence of strongly coupled nuclear spin that suppress other nuclei. By sweeping τ_1 and τ_2 , one can go through different bright and blind spots of each nuclear spin, observe which two peaks are correlated.

Appendix C: DD analysis for bispecies systems

Consider a single color center that is surrounded by two nuclear spin species. Each species has a distinct bath, which is processing with its corresponding Larmor frequency. Assuming large Larmor frequency with respect to hyperfine couplings, one can write Eq. 6 for two bath ($\omega_0 \approx \omega_1 \approx \omega_L$) as follows:

$$\langle \sigma_z \rangle_{\text{bath}} \approx 1 - 2k_1^2 \sin^4\left(\frac{\omega_L^{(1)} \tau}{2}\right) - 2k_2^2 \sin^4\left(\frac{\omega_L^{(2)} \tau}{2}\right) \quad (\text{C1})$$

This means that two baths interfere, and the periodicity of the total bath is not straightforward any more. Hence, if there is a narrow peak next in DD signal, it can be attributed to both of the baths. To clarify the type of nuclear spins, one has to perform further experiments, e.g., in various external magnetic fields.

-
- [1] D. D. Awschalom, R. Hanson, J. Wrachtrup, and B. B. Zhou, Quantum technologies with optically interfaced solid-state spins, *Nature Photonics* **12**, 516 (2018).
 - [2] M. Pompili, S. L. Hermans, S. Baier, H. K. Beukers, P. C. Humphreys, R. N. Schouten, R. F. Vermeulen, M. J. Tiggelman, L. dos Santos Martins, B. Dirkse, *et al.*, Realization of a multinode quantum network of remote solid-state qubits, *Science* **372**, 259 (2021).
 - [3] C. L. Degen, F. Reinhard, and P. Cappellaro, Quantum sensing, *Reviews of modern physics* **89**, 035002 (2017).
 - [4] C. E. Bradley, J. Randall, M. H. Abobeih, R. Berrevoets, M. Degen, M. A. Bakker, M. Markham, D. Twitchen, and T. H. Taminiau, A ten-qubit solid-state spin register with quantum memory up to one minute, *Physical Review X* **9**, 031045 (2019).
 - [5] L. Childress, M. Gurudev Dutt, J. Taylor, A. Zibrov, F. Jelezko, J. Wrachtrup, P. Hemmer, and M. Lukin, Coherent dynamics of coupled electron and nuclear spin qubits in diamond, *Science* **314**, 281 (2006).
 - [6] M. Abobeih, J. Randall, C. Bradley, H. Bartling, M. Bakker, M. Degen, M. Markham, D. Twitchen, and T. Taminiau, Atomic-scale imaging of a 27-nuclear-spin cluster using a quantum sensor, *Nature* **576**, 411 (2019).
 - [7] B. Kasumaj and S. Stoll, 5-and 6-pulse electron spin echo envelope modulation (eseem) of multi-nuclear spin systems, *Journal of Magnetic Resonance* **190**, 233 (2008).
 - [8] V. Vorobyov, J. Javadzade, M. Joliffe, F. Kaiser, and J. Wrachtrup, Addressing single nuclear spins quantum memories by a central electron spin, *Applied Magnetic Resonance* **53**, 1317 (2022).
 - [9] S. Stoll, C. Calle, G. Mitrikas, and A. Schweiger, Peak suppression in esem spectra of multinuclear spin systems, *Journal of Magnetic Resonance* **177**, 93 (2005).